

Noncoding RNAs-based high KIF26B expression correlates with poor prognosis and tumor immune infiltration in colon cancer

Zhihong Liu ^{a*}, Xin Zhou^{a*}, Bo Chen^{b*}, Ziyu Wu^a, Cuifeng Zhang^a, Changji Gu^a, Juan Li^c, and Xiaodong Yang ^a

^aDepartment of General Surgery, The Second Affiliated Hospital of Soochow University, Suzhou, China; ^bNursing Department, The Second Affiliated Hospital of Soochow University, Suzhou, China; ^cDepartment of Gastroenterology, The Second Affiliated Hospital of Soochow University, Suzhou, China

ABSTRACT

Background: The protein kinesin family member 26B (KIF26B) is aberrantly expressed in various cancers. However, its particular role and association with tumor immune infiltration in colon adenocarcinoma (COAD) remain unclear.

Methods: All original data were downloaded directly from The Cancer Genome Atlas (TCGA), UCSC Xena, and Gene Expression Omnibus (GEO) databases and processed with R 3.6.3. KIF26B expression was analyzed using OncoPrint, TIMER, TCGA, GEO databases, and our clinical specimens. KIF26B expression at the protein level was explored with Human Protein Atlas (HPA) database. The upstream miRNAs and lncRNAs were predicted by StarBase and validated using RT-qPCR. Correlation of KIF26B expression with the expression of immune-related or immune checkpoint genes and GSEA analysis of KIF26B-related genes were investigated via R software. Relationship of KIF26B expression with immune biomarkers or tumor immune infiltration levels was studied through GEPIA2 and TIMER databases.

Results: KIF26B was upregulated, and its overexpression was closely related to overall survival (OS), disease-specific survival (DSS), progression-free interval (PFI), T stage, N stage, and CEA levels in COAD. MIR4435-2HG/hsa-miR-500a-3p/KIF26B axis was identified as the promising regulatory pathway of KIF26B. KIF26B expression was positively correlated with immune-related genes, tumor immune infiltration, and biomarker genes of immune cells in COAD, and KIF26B-related genes were significantly enriched in macrophage activation-related pathways. Expression of immune checkpoint genes, including PDCD1, CD274, and CTLA4, was also closely related to KIF26B expression.

Conclusions: Our results clarified that ncRNA-based increased KIF26B expression was associated with a worse prognosis and high tumor immune infiltration in COAD.

ARTICLE HISTORY

Received 2 February 2023

Revised 23 March 2023

Accepted 27 March 2023

KEYWORDS

KIF26B; prognostic value; immune cell infiltration; biomarkers; immune checkpoints

1. Introduction


Colorectal cancer (CRC), including colon adenocarcinoma and rectum adenocarcinoma, is a highly heterogeneous disease and one of the deadliest primary malignant neoplasms. According to new global statistics, CRC is still the third most common tumor and the second leading cause of tumor-associated mortality [1]. With improvements in medical technology for early detection, the overall incidence of CRC has shown a continuous decline since the 2000s. In contrast, the incidence rate increased obviously among individuals younger than 50 years of age [2]. In addition, most CRC

patients are diagnosed at an advanced stage because it is largely an asymptomatic disease [3]. Thus, it is urgent and essential to identify molecular biomarkers for early diagnosis and improve treatment effects.

The Kinesin superfamily proteins (KIFs), expressed in all eukaryotes, are a series of proteins that have a highly conserved motor domain. To date, 45 kinesin proteins have been identified and are divided into 14 different families [4]. It has previously been observed that KIFs can transport intracellular components such as organelles, protein complexes, and mRNAs to specific destinations

CONTACT Xiaodong Yang  yangxiaodong2366@suda.edu.cn; wjyxd@163.com  Department of General Surgery, The Second Affiliated Hospital of Soochow University, Suzhou, Jiangsu Province 215004, China; Juan Li  lijuan2369@suda.edu.cn; suzhouzhengheng@126.com  Department of Gastroenterology, The Second Affiliated Hospital of Soochow University, Suzhou, Jiangsu Province 215004, China

*These authors have contributed equally to this work.

 Supplemental data for this article can be accessed online at <https://doi.org/10.1080/15384101.2023.2222520>

© 2023 The Author(s). Published by Informa UK Limited, trading as Taylor & Francis Group.

This is an Open Access article distributed under the terms of the Creative Commons Attribution-NonCommercial-NoDerivatives License (<http://creativecommons.org/licenses/by-nc-nd/4.0/>), which permits non-commercial re-use, distribution, and reproduction in any medium, provided the original work is properly cited, and is not altered, transformed, or built upon in any way. The terms on which this article has been published allow the posting of the Accepted Manuscript in a repository by the author(s) or with their consent.

in a microtubule- and ATP-dependent manner [5–7]. In addition to participating in intracellular transport, KIFs can also regulate the movements of chromosomes and spindles during mitosis and meiosis [8–10]. In recent years, many studies have indicated that KIFs play a vital role in the initiation and progression of many human malignancies [11–13]. Therefore, further exploration of the biological functions of kinesin proteins may promote the identification of indicators for early detection, diagnosis, prognostic assessment, and even molecular-targeting treatment for tumors.

The KIF26B gene, located on chromosome 1q44, belongs to the KIF family and consists of 2108 amino acids [14]. It has been reported that KIF26B can regulate adhesion and polarization between mesenchymal cells and ureteric buds, and its posttranslational modification and degradation play a critical role in the developing kidney [15,16]. Recent research has demonstrated that KIF26B is associated with the tumorigenesis, progression, and metastasis of many solid tumors, including breast cancer [17–19], liver cancer [20], and gastric cancer [21]. Reports have indicated that KIF26B is an independent prognostic biomarker and perhaps a potential therapeutic indicator for CRC patients [22]. However, the biological function and molecular regulatory mechanism of KIF26B in COAD have not been fully explored. Moreover, the relationship between KIF26B and tumor immune infiltration in COAD remains to be elucidated.

In our research, we first analyzed KIF26B expression in different tumor types. To evaluate the prognostic and clinical value of KIF26B in COAD, we explored the association of KIF26B expression with clinicopathological parameters. Next, the regulatory network of KIF26B in COAD was established, including lncRNAs and miRNAs. Moreover, relevance analysis was carried out between immune-related genes and KIF26B in multiple human cancers. Finally, we investigated the association of KIF26B expression with tumor immune cell infiltration levels, immune cell biomarkers, and immune checkpoints in COAD. In summary, our study indicates that ncRNA-induced overexpression of KIF26B is closely associated with adverse prognosis and high tumor immune infiltration in COAD.

2. Materials and methods

2.1 Raw data download, process, and analysis

Fragments per kilobase million (FPKM) gene-level data (containing 480 COAD specimens and 41 normal tissue specimens) were downloaded from the TCGA database (<https://portal.gdc.cancer.gov/>). Then, we converted these values to transcripts per million (TPM) using R (version 3.6.3) [23]. Pan-cancer normalized gene expression data were downloaded from the UCSC Xena platform (<https://xena.ucsc.edu/>). We also downloaded external gene expression profiles from the GEO database (<https://www.ncbi.nlm.nih.gov/geo/>): GSE9348 (containing 70 COAD specimens and 12 normal specimens), GSE35279 (containing 74 COAD specimens and 5 normal tissue specimens), GSE21815 (containing 132 COAD specimens and 9 normal tissue specimens), GSE41328 (containing 10 COAD specimens and 10 matched normal tissue specimens), GSE110224 (containing 17 COAD specimens and 17 matched normal tissue specimens) and GSE41657 (containing 12 normal mucosae, 21 low-grade adenomas, 30 high-grade adenomas, and 25 adenocarcinomas). These datasets were used to further validate our results. Meanwhile, KIF26B expression at the protein level was confirmed in COAD via the HPA database (<https://www.proteinatlas.org/>), which was an open and free platform that provides scientists with valuable information about the expression and localization of proteins in human tissues, cells, and organs [24,25].

2.2 Oncomine

Oncomine database, a gene chip-based database, is available at <https://www.oncomine.org/resource/login.html> [26]. KIF26B transcription levels in different tumor types were determined by Oncomine. We chose 0.05 and 1.5 as thresholds for p -value and fold change, respectively.

2.3 TIMER

TIMER (<http://timer.cistrome.org/>) is a comprehensive tool that provides free systematic analysis of tumor-infiltrating immune cells. It provides a more

robust estimation of immune infiltration levels for TCGA and visualization functions of tumor-infiltrating immune cells. In our study, TIMER was used to explore KIF26B expression in normal specimens and tumor specimens in various human malignancies and analyze the correlation of KIF26B expression or somatic copy number alterations (sCNAs) with immune cell infiltration levels. Genes with sCNAs are hallmarks of tumorigenesis and progression and could influence immunotherapy response [27,28]. We compared immune infiltration distribution by the sCNA status of KIF26B in COAD.

2.4 GEPIA2

GEPIA2 (<http://gepia2.cancer-pku.cn/#index>) is an online database for profiling and interactive analysis of normal and cancer gene expression [29]. We used GEPIA2 to look at the relationship between KIF26B transcription levels and OS. Simultaneously, GEPIA2 was used to explore the association between KIF26B expression and immune cell biomarkers. In addition, $|r| > 0.1$ and p -value < 0.05 were regarded as significantly correlated.

2.5 Candidate miRNA prediction

The possible upstream miRNAs binding to KIF26B were forecasted through miRNA target prediction tools, including PITA [30], microT [31], miRanda [32], miRmap [33], PicTar [34], RNA22 [35], and TargetScan [36]. The target miRNAs should be predicted by mRNA from at least two different prediction programs as mentioned above. These selected miRNAs were considered promising upstream miRNAs of KIF26B. $R < -0.2$ and $p < 0.05$ were used as the criteria for screening ideal miRNA.

2.6 StarBase

StarBase (<https://starbase.sysu.edu.cn/>) is an interactive platform for searching the ncRNA-mRNA interaction map database [37]. We performed correlation analysis on the expression of miRNA-KIF26B, lncRNA-hsa-miR-500a-3p, and lncRNA-KIF26B in COAD. Differential gene expression analysis of hsa-miR-500a-3p and MIR4435-2HG in COAD specimens and normal tissue specimens

was also investigated through StarBase. In addition, potential lncRNAs that might bind to hsa-miR-500a-3p were predicted using the StarBase database. $R < -0.1$ and $p < 0.05$ were used as the criteria for screening ideal lncRNA.

2.7 KIF26B-related gene GSEA analysis

KIF26B-related gene GSEA analysis was conducted for investigating the correlation between KIF26B and macrophage polarization-related pathways. We extracted the expression of KIF26B in COAD from the TCGA database and then correlated it with the expression of the remaining other genes separately. Correlation analysis was carried out using Pearson correlation analysis. Based on the results of the correlation analysis, genes were sorted by correlation coefficient and their correlation coefficients were used to perform GSEA enrichment analysis. Clusterprofiler and ggplot2 packages were used for GSEA enrichment analysis and visualization [38,39]. Hallmark gene sets were selected as the reference gene set.

2.8 Cell culture and cell transfection

Human-derived colon cancer cell lines (HT29 and HCT116) were cultured in DMEM or Mocoey's 5A supplemented with 10% FBS and 1% penicillin/streptomycin, and incubated at 37°C humidified atmosphere with 5% CO₂. The HT29 and HCT116 cell lines were cultured in a 6-well plate to 70–80% confluence. Cell transfection was performed using Lipofectamine 2000 (Invitrogen, USA) based on the instructions. RNA was extracted from the cells 24 hours after transfection. Hsa-miR-500a-3p mimics and its corresponding primer were purchased from RIBOBIO (Guangzhou, China).

2.9 Human tissue samples

Between June 2020 and December 2021, 12 paired tumors and their companion normal tissue specimens from patients with COAD were collected at the Gastrointestinal Surgery Department of the Second Affiliated Hospital of Soochow University. All tissue specimens were quick-frozen after surgical resection and stored at -80°C until RNA extraction.

2.10 Immunohistochemical staining

Tissue microarrays (TMA) of colorectal cancer tissue and normal tissue were used for immunohistochemistry (IHC) staining. Tissue sections were placed in the oven for 1 h and then dewaxed and hydrated. Antigen retrieval was achieved by microwave using sodium citrate antigen-retrieval solution (#C1032, Solarbio, Beijing, China). After natural cooling, endogenous peroxidase activity was blocked with endogenous peroxidase blocking solution for 10 min. Tissue sections were washed three times with PBS, and serum blocking was performed with a 5% normal goat serum solution for 1 h at RT. Then, tissue sections were incubated overnight with primary antibody for KIF26B (1:1000 dilution, #17422, Proteintech, Chicago, IL, USA), CD163 (1:1000 dilution, #16646, Proteintech, Chicago, IL, USA) and CCL2 (1:1000 dilution, #25542, Proteintech, Chicago, IL, USA) at 4°C separately. After washing with PBST, each section was incubated with Biotinylated Goat anti-Mouse & Rabbit IgG (H+L) (#SP9000, ZSGB-BIO, China) for 1 h at room temperature. Tissue sections were washed with PBST, and each section was incubated with streptavidin-conjugated horseradish peroxidase (HRP) solution for 10 min. DAB solution (#ZLI-9017, ZSGB-BIO, China) was used for the DAB chromogenic reaction. Cell nuclei were stained with hematoxylin for 3 min (#G1080, Solarbio, Beijing, China). After dehydration and sealing piece with neutral gum, sections were detected and photographed by microscope. According to the result, patients were divided into high and low-expression groups. Finally, we statistically analyze the respective frequencies and calculate the correlation between KIF26B and CD163 or CCL2.

2.11 qRT-PCR

RNAiso Plus (TaKaRa, Tokyo, Japan) was used to extract total RNA from the clinical tissue specimens. PrimeScript™ RT reagent Kit was used to perform synthesization of First-strand cDNA (TaKaRa, Tokyo, Japan). Quantitative RT-PCR (qRT-PCR) was conducted by FastStart Universal SYBR Green Master (Rox) (Roche, Mannheim, Germany) on a CFX96™ Real-Time PCR machine (BIO-RAD). Genes and matched primer sequences were listed in **Table S1**.

2.12 Statistical analysis

KIF26B expression in COAD specimens was evaluated by boxplots and line graphs. The correlation of KIF26B expression with clinical parameters was evaluated by Wilcoxon rank-sum test. The best cut-off value of gene expression was used to perform survival analysis. Log-rank test was used to analyze the significant difference in the survival curve. Pearson coefficient was utilized to evaluate the relationship of KIF26B expression with immune checkpoints expression. The regulatory network was established via Cytoscape (version 3.8.2). Limma and survival packages were used to process raw data. Survminer and ggplot2 packages were used to perform visualization. In all analyses, *, **, and *** indicated $p < 0.05$, $p < 0.01$ and $p < 0.001$, respectively.

3. Results

3.1 KIF26B expression in pan-cancer

We first assessed KIF26B transcript levels across cancers through Oncomine. These results revealed that compared with that in respective normal specimens, KIF26B expression was upregulated in tumor specimens, including bladder, breast, colorectal, gastric, kidney, and lung cancers, lymphoma, and sarcoma. Meanwhile, downregulated expression of KIF26B was only discovered in one kidney malignancy dataset (**Figure 1a**).

To further assess KIF26B transcript levels in various types of cancer, we investigated RNA sequencing data from TCGA using TIMER. As demonstrated in **Figure 1b**, compared with normal controls, KIF26B was increased in 17 tumor types, including BRCA, BLCA, COAD, CHOL, ESCA, HNSC, HNSC-HPV positive, LIHC, LUSC, LUAD, READ, STAD, and UCEC, and was markedly decreased in 4 tumor types, including KICH, KIRC, PPAD, and THCA. Next, we investigated KIF26B expression in COAD samples and compared them with corresponding normal controls. Results indicated that KIF26B expression was increased in unpaired samples (**Figure 1c**) and paired samples (**Figure 1d**). To further explore the role of KIF26B in the progression of colon cancer, we analyzed KIF26B expression in normal mucosae, low-grade adenomas, high-grade adenomas, and

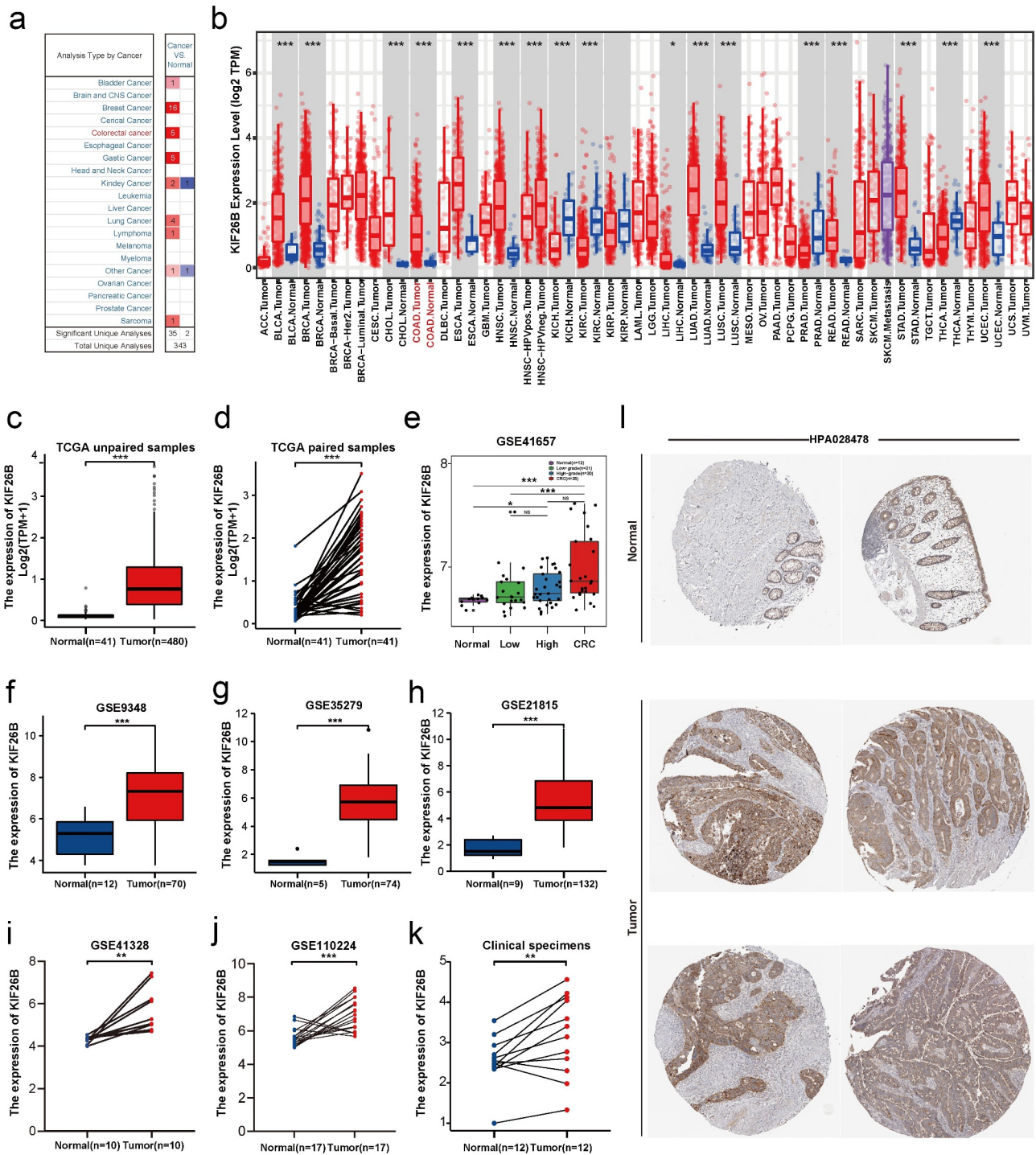


Figure 1. Aberrant expression of KIF26B in different tumors. (a) Increased or decreased KIF26B expression in datasets of various cancers compared with normal tissues in OncoPrint (threshold: fold change 1.5, p-value 0.05). (b) KIF26B expression in diverse tumor and normal tissues were detected using TIMER. (c-d) KIF26B expression in colon tumors and unpaired normal tissues or paired normal tissues of TCGA datasets. (e) KIF26B expression between normal mucosae, low-grade adenomas, high-grade adenomas, and adenocarcinomas in GSE41657. (f-h) Expression of KIF26B in tumor and unpaired normal tissues of GSE9348, GSE35279, and GSE21815 datasets. (i-j) KIF26B expression in tumor and paired adjacent tissues in GSE41328 and GSE110224 datasets. (k) KIF26B expression in COAD. (l) Validate the increased expression of KIF26B in COAD by HPA.

adenocarcinomas using GSE41657, and its expression was found to increase progressively with tumor progression (Figure 1e). To confirm KIF26B expression in COAD, we chose another five independent GEO datasets that served as validation sets, including three unpaired datasets (GSE9348, GSE35279, and GSE21815) and two paired datasets (GSE41328 and GSE110224). These results also suggested higher KIF26B transcript levels in tumor tissues than in normal epithelial tissues (Figure 1f-j). Moreover, we validated this outcome using 12 pairs of clinical samples ($p < 0.01$) (Figure 1k). Furthermore, the KIF26B protein expression level was examined in COAD based on the HPA database. These results also suggested that KIF26B expression was upregulated in tumor specimens compared with normal controls (Figure 1l).

3.2 The prognostic values of KIF26B in COAD

To assess prognostic and clinical values for COAD, we investigated KIF26B expression among groups of patients in accordance with different clinical parameters. Our results showed that upregulated KIF26B expression was closely

related to T stage ($p = 0.018$), N stage ($p = 0.038$), and CEA level ($p = 0.04$). In contrast, there was no significant difference between KIF26B expression and M stage ($p = 0.081$) (Figure 2a-d). We performed survival analysis to further assess the prognostic value of KIF26B expression. The results indicated that increased KIF26B expression was closely correlated with OS ($p = 0.032$), DSS ($p = 0.006$), and PFI ($p = 0.001$) (Figure 2e-g). Then, we also validated the prognostic value of KIF26B in COAD by GEPIA2 ($p = 0.017$).

3.3 Prediction analysis of the upstream miRNAs of KIF26B

To explore the regulatory network of KIF26B, upstream miRNAs were predicted by StarBase, and we found 31 miRNAs that could potentially bind to KIF26B. We established a miRNA-KIF26B regulatory network for better presentation through Cytoscape (Figure 3a). Candidate miRNAs that negatively correlated with KIF26B expression were filtered for subsequent analysis. Then, we performed a correlation analysis between the

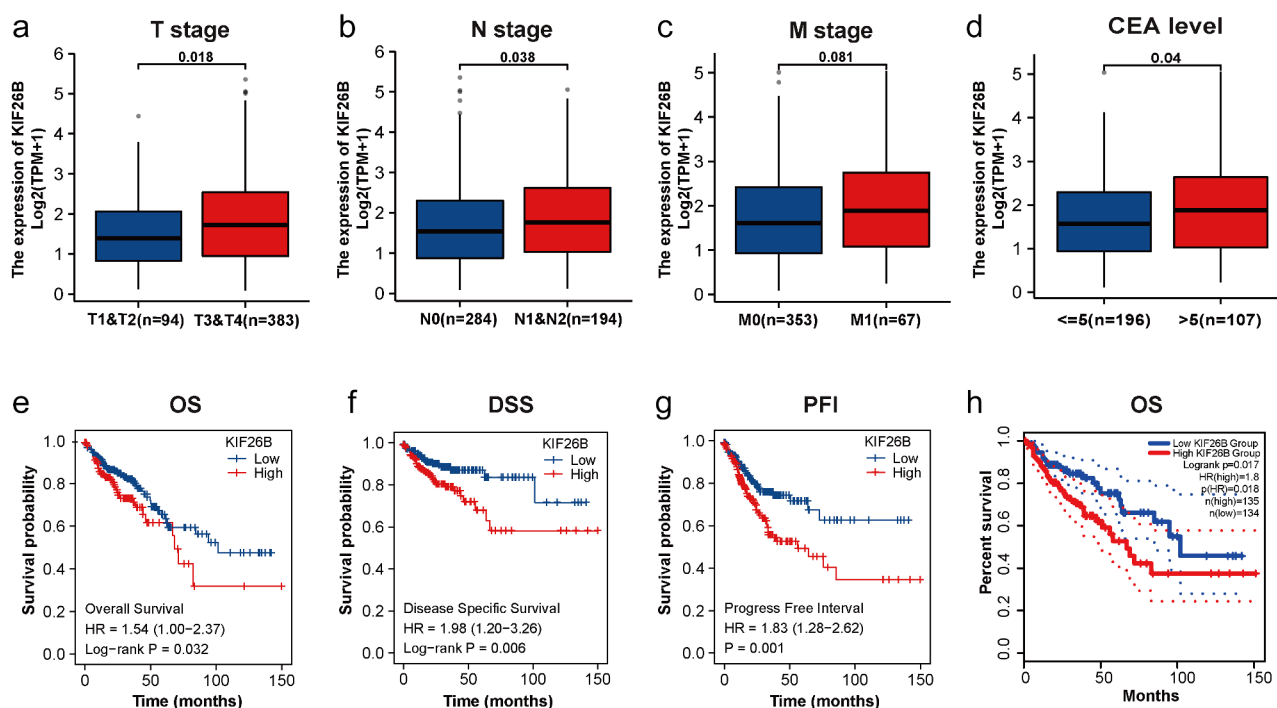


Figure 2. The prognostic value of KIF26B in COAD. (a-d) Difference analysis between KIF26B expression and clinicopathological factors, including T stage ($p = 0.018$), N stage ($p = 0.038$), M stage ($p = 0.081$), and CEA levels ($p = 0.04$). (e-g) Kaplan–Meier survival curves for OS, DSS, and PFI of KIF26B in COAD via R software. (h) Kaplan–Meier survival curves for OS by GEPIA2.

expression of predicted miRNAs and KIF26B. As listed in Table 1, we finally found six miRNAs that met our requirements ($r < -0.2$, $p < 0.05$), of which only hsa-miR-500a-3p and hsa-miR-93-5p were decreased in COAD. Nevertheless, no significant difference was found in hsa-miR-93-5p expression between normal and tumor tissues. Finally, analysis of differential gene expression and survival

analysis were carried out for hsa-miR-500a-3p in COAD. As described in Figure 3b,c, hsa-miR-500a-3p was profoundly downregulated both in unpaired ($p < 0.001$) and paired ($p < 0.01$) tissue samples from TCGA database, and we verified this finding using StarBase ($p < 0.001$) (Figure 3d). Correlation analysis between KIF26B expression and hsa-miR-500a-3p was also validated by

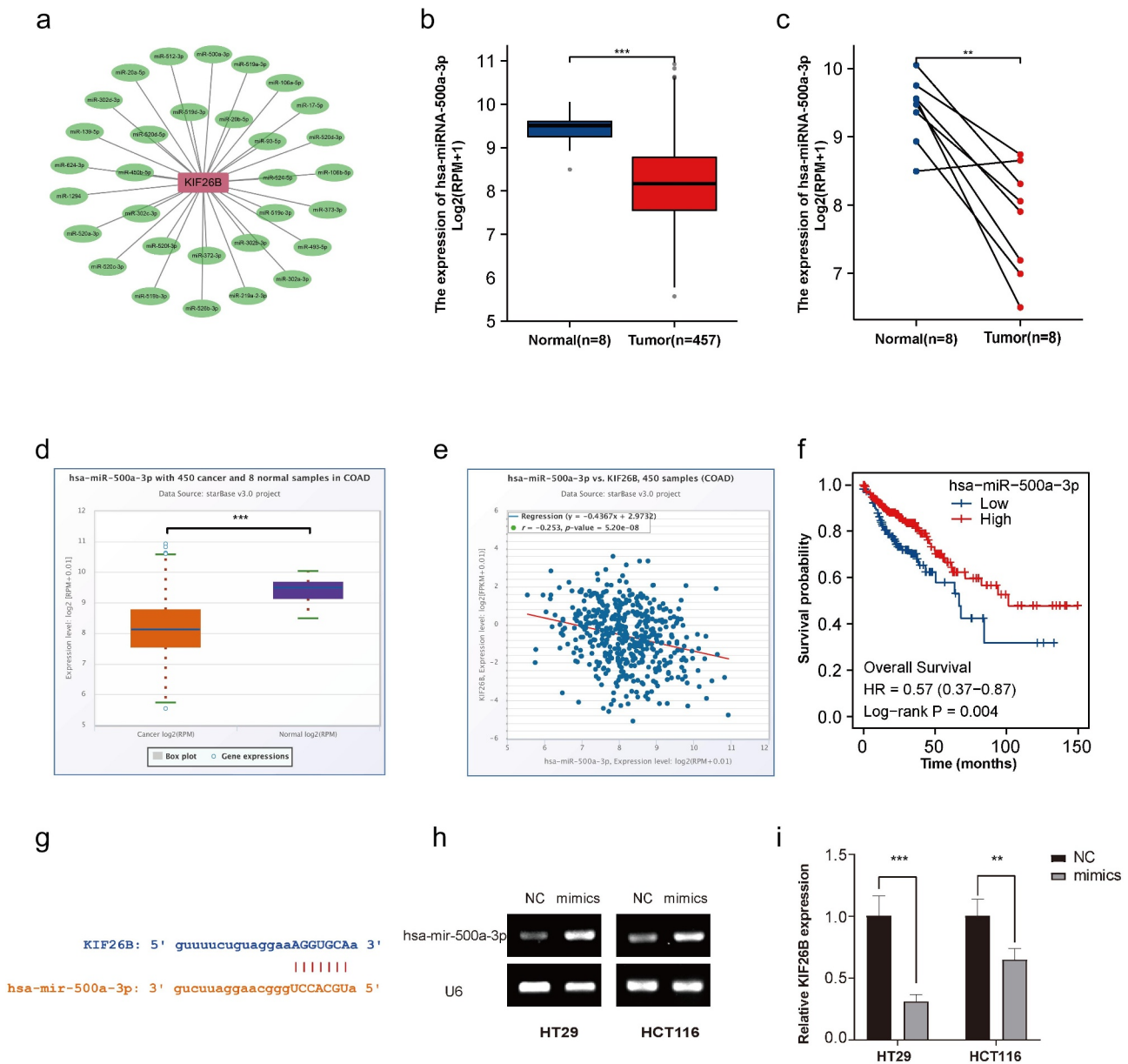


Figure 3. Identification of hsa-miR-500a-3p as a potential upstream miRNA of KIF26B in COAD. (a) The miRNA-KIF26B regulatory network was conducted using Cytoscape. (b-c) The expression of hsa-miR-500a-3p in colon tumor tissues and unpaired normal tissues or paired normal tissues. (d) Validation of the differently expressed of hsa-miR-500a-3p by StarBase. (e) Correlation analysis between hsa-miR-500a-3p and KIF26B expression by StarBase. (f) Evaluate the prognostic value of hsa-miR-500a-3p. (g) Base pairing between hsa-miR-500a-3p and the target site in the KIF26B 3' UTR predicted by StarBase. (h) Validation of mimics transfection efficiency in HT29 and HCT116 cell lines by agarose gel electrophoresis experiments. (i) Suppression of target gene KIF26B by hsa-miR-500a-3p mimics by RT-qPCR.

Table 1. The correlation analysis between KIF26B expression and potential miRNAs in COAD by R software (correlation threshold: $r < -0.2$, $p < 0.05$).

Gene	miRNA	r value	p value	logFC	diffPval
KIF26B	hsa-miR-106b-5p	-0.366	1.17E-15	4.58	1.23E-06
KIF26B	hsa-miR-17-5p	-0.315	1.04E-11	3.34	1.89E-06
KIF26B	hsa-miR-106a-5p	-0.273	4.34E-09	2.55	3.37E-05
KIF26B	hsa-miR-500a-3p	-0.247	1.22E-07	-1.19	3.18E-04
KIF26B	hsa-miR-20a-5p	-0.227	1.24E-06	4.57	1.25E-06
KIF26B	hsa-miR-93-5p	-0.220	2.65E-06	-0.18	4.58E-01

this database ($r = -0.253$, $p = 5.20e-08$) (Figure 3e). Similarly, negative relationship of hsa-miR-500a-3p expression with patient prognosis ($p = 0.004$) was found in COAD (Figure 3f). To clarify the regulatory role of miRNAs on KIF26B, the target sites in KIF26B 3' UTRs were predicted to pair with hsa-miR-500a-3p by Starbase (Figure 3g). Then, we verified the inhibitory effect of hsa-miR-500a-3p on KIF26B by transfection experiment. Hsa-miR-500a-3p was significantly overexpressed in both HT29 and HCT116 cell lines after transfection (Figure 3h). As predicted, KIF26B expression was significantly down-regulated after transfection (Figure 3i).

3.4 Prediction analysis of the upstream lncRNAs of hsa-miR-500a-3p

We further forecasted lncRNAs as potential hsa-miR-500a-3p precursors by StarBase and found 27 possible lncRNAs. Similarly, for better presentation, a lncRNA-hsa-miR-500a-3p regulatory network was constructed (Supplemental Figure 1a). In accordance with the competing endogenous RNAs hypothesis, candidate lncRNAs can upregulate target mRNAs expression by sponging to competitively bind to shared miRNAs. Therefore, ideal lncRNAs should be correlated with miRNAs negatively or positively related to mRNAs, and only two lncRNAs satisfied this screening criterion ($r < -0.1$, $p < 0.05$) (Table 2). Then, we conducted difference analysis and survival analysis for candidate lncRNAs,

and our results showed that both DLGAP1-AS5 (Supplemental Figure 1b,c) and MIR4435-2HG (Figure 4a,b) were upregulated in unpaired and paired samples from TCGA database ($p < 0.01$). Survival analysis results showed that increased MIR4435-2HG transcript level predicted a worse prognosis ($p = 0.004$) (Figure 4c), while there was no significant difference between DLGAP1-AS5 expression and survival time ($p = 0.471$) (Supplemental Figure 1d). Furthermore, we verified upregulated expression of MIR4435-2HG in COAD via StarBase ($p < 0.05$) (Figure 4d). Finally, we confirmed the correlation between the transcript levels of MIR4435-2HG and hsa-miR-500a-3p ($r = -0.137$, $p = 3.47e-03$) (Figure 4e) or KIF26B ($r = 0.462$, $p = 2.93e-26$) (Figure 4f) using StarBase. To clarify the regulatory role of miRNAs on MIR4435-2HG, the target sites in MIR4435-2HG 3' UTRs were predicted to pair with hsa-miR-500a-3p by StarBase (Figure 4g). Also, we found that MIR4435-2HG expression was significantly down-regulated after transfection (Figure 4h). Finally, we summarized the role of miRNAs in the MIR4435-2HG/hsa-miR-500a-3p/KIF26B axis (Figure 4i).

3.5 Positive correlation of KIF26B and immune cell infiltration in COAD

In tumor patients, immune cell tumor infiltration levels can affect lymph node metastasis and survival. We first performed gene co-expression

Table 2. The relationship of upstream lncRNAs expression with hsa-miR-500a-3p or KIF26B expression in COAD by R software (correlation threshold: $r < -0.1$, $p < 0.05$).

lncRNA	miRNA	r value	p value	logFC	diffPval
DLGAP1-AS5	hsa-miR-500a-3p	-0.111	1.86E-02	0.37	8.93E-03
MIR4435-2HG	hsa-miR-500a-3p	-0.182	1.05E-04	1.27	9.48E-23
DLGAP1-AS5	KIF26B	0.094	4.58E-02	0.37	8.93E-03
MIR4435-2HG	KIF26B	0.475	<2.2E-16	1.27	9.48E-23

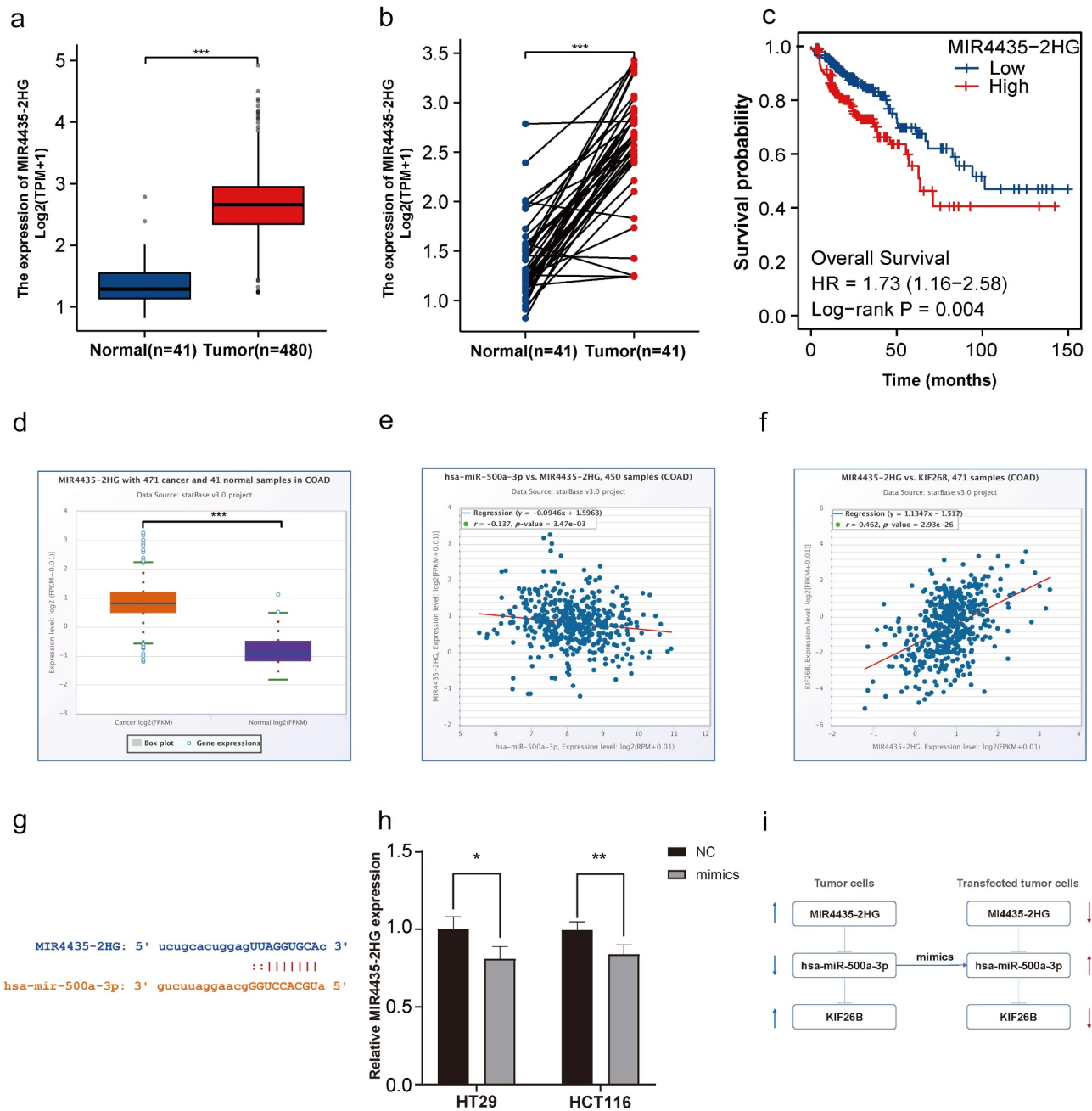


Figure 4. Expression and survival analysis for upstream lncRNAs of hsa-miR-500a-3p in COAD. (a-b) MIR4435-2HG expression in colon tumor tissues and unpaired normal tissues or paired normal tissues. (c) Kaplan-Meier survival curve analysis for OS of MIR4435-2HG in COAD. (d) Validation of the MIR4435-2HG expression between tumor and normal tissues by StarBase. (e-f) Correlation between the expression of MIR4435-2HG and hsa-miR-500a-3p or KIF26B using StarBase. (g) Base pairing between hsa-miR-500a-3p and the target site in the MIR4435-2HG 3' UTR predicted by StarBase. (h) Suppression of target gene MIR4435-2HG by hsa-miR-500a-3p mimics by RT-qPCR. (i) Schematic model of the regulatory role of hsa-miR-500a-3p mimics.

analyses to examine the links of KIF26B expression with immune-associated genes in all types of tumors. The selected gene set encoded chemokine receptor (Figure 5a), chemokine (Figure 5b), immunosuppressive (Figure 5c), and immune activation protein (Figure 5d). The correlation

heatmap illustrated that KIF26B was co-expressed with almost all immune-related genes, and within all types of tumors, the majority were positively correlated with KIF26B expression, especially COAD ($p < 0.05$). Furthermore, we analyzed the relationship of KIF26B expression

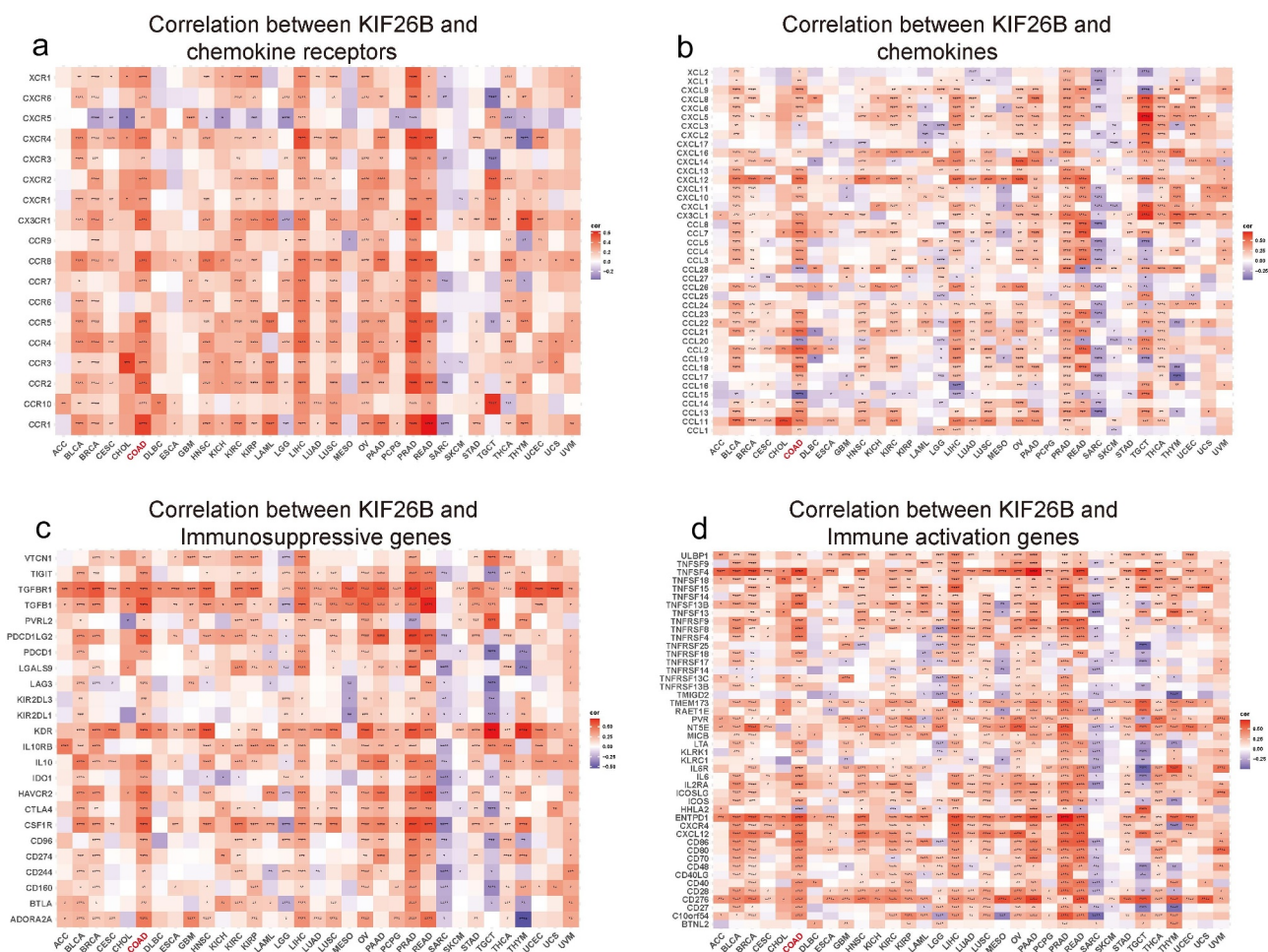


Figure 5. Correlation analysis between KIF26B expression and immune-related gene expression in various tumors. (a) chemokine receptors. (b) chemokines. (c) immunosuppressive genes. (d) immune activation genes.

with the degree of tumor-infiltrating lymphocytes by the TIMER database. As presented in [Figure 6a](#), significant copy number changes were observed in B cells, CD8+ T cells, and dendritic cells, while no noticeable changes were found in CD4+ T cells, macrophages, or neutrophils. To further investigate the biological function and molecular mechanism of action of KIF26B, we estimated the relevance of KIF26B expression to immune cell infiltration levels. As described in [Figure 6b–g](#), KIF26B expression was positively connected with most of the selected immune cells, including CD8+ T cells ($r = 0.156$, $p = 1.57e-03$), CD4+ T cells ($r = 0.403$, $p = 3.86e-17$), macrophages ($r = 0.461$, $p = 1.06e-12$), neutrophils ($r = 0.366$, $p = 3.65e-14$) and dendritic cells ($r = 0.355$, $p = 2.16e-13$) in COAD, while KIF26B in B cells had no obvious link.

3.6 Assessment of the relevance of KIF26B expression to immune markers

To further explore the association of KIF26B expression with immune cell infiltration levels, relevance analysis was conducted between KIF26B expression and immunological markers of tumor-associated macrophages (TAMs), M1 macrophages, M2 macrophages, and monocytes in COAD by TIMER and GEPIA2. After adjusting according to tumor purity, we found that KIF26B expression was positively associated with that of the majority of monocyte markers (CD86, CSF1R) ([Figure 7a](#)), TAM markers (CCL2, IL10) ([Figure 7b](#)), M1 macrophage markers (PTGS2, IRF5, NOS2) ([Figure 7c](#)), and M2 macrophage markers (CD163, MS4A4A, VSIG4) ([Figure 7d](#)) in COAD. In contrast, only NOS2+ M1 macrophages were negatively correlated with KIF26B in

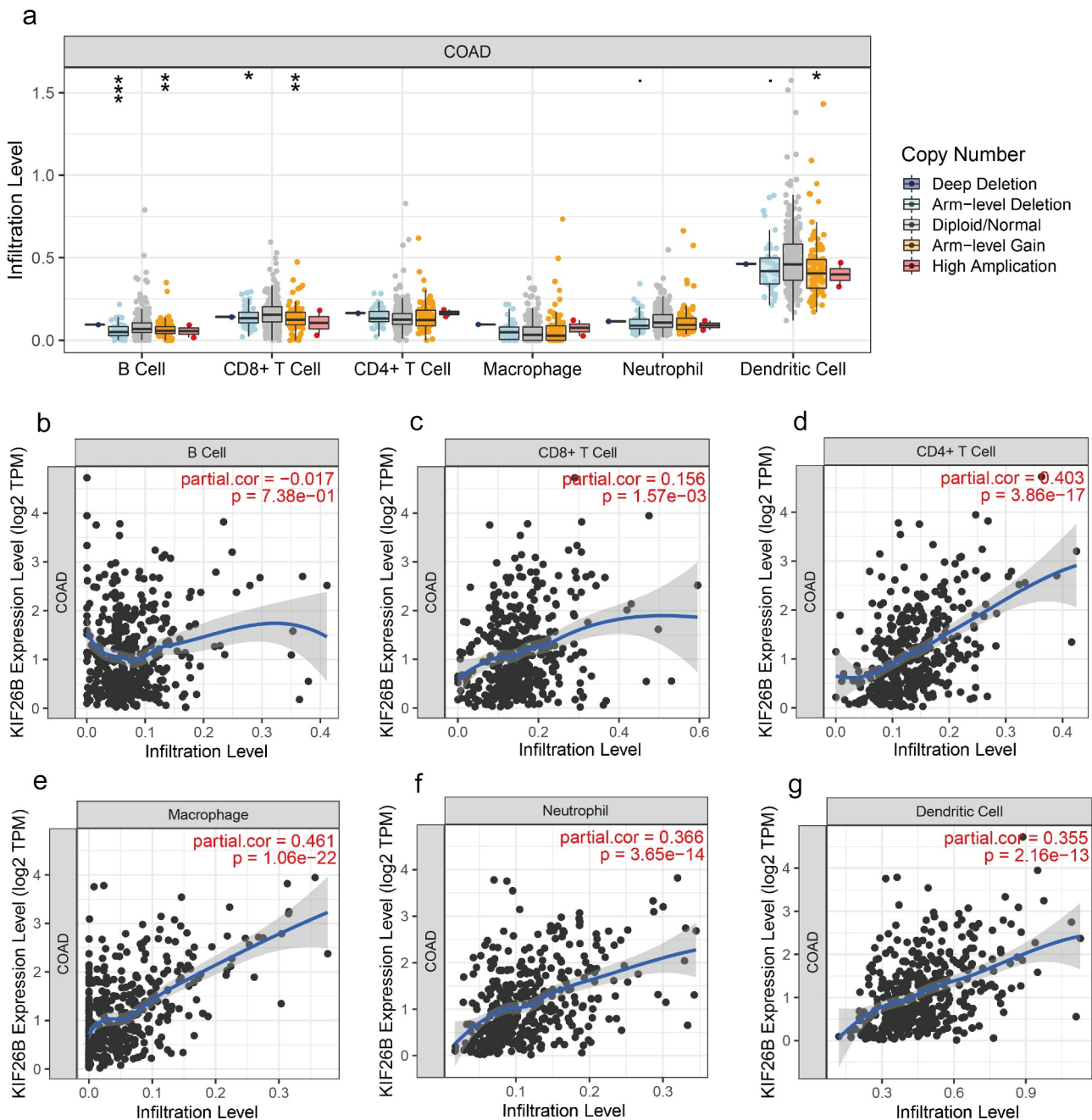


Figure 6. Correlation between immune cell infiltration and KIF26B expression in COAD. (a) Association between various copy numbers of KIF26B and infiltration levels of different immune cells. (b-g) Scatterplots of correlations between KIF26B expression and the infiltration levels of B cell (b), CD8+ T cell (c), CD4+ T cell (d), Macrophage (e), Neutrophil (f), and Dendritic cell (g).

COAD. To confirm these results, we assessed the association of KIF26B expression with these markers in COAD via GEPIA2 and drew similar conclusions. As depicted in Table 3, in tumor tissues, KIF26B expression correlated significantly with all listed immune cell markers, however, in normal tissues KIF26B expression only correlated statistically with the expression of CCL2 and PTGS2

genes. Then, we performed single gene correlation analysis and ranked the genes by correlation coefficient, and performed GSEA. As shown in Figure 7e, KIF26B-related genes were significantly enriched in macrophage polarization-related pathways including IL6-JAK-STAT3 signal pathway, notch signal pathway, PI3K-AKT-MTOR signal pathway, and TNFA signal via NFKB pathway.

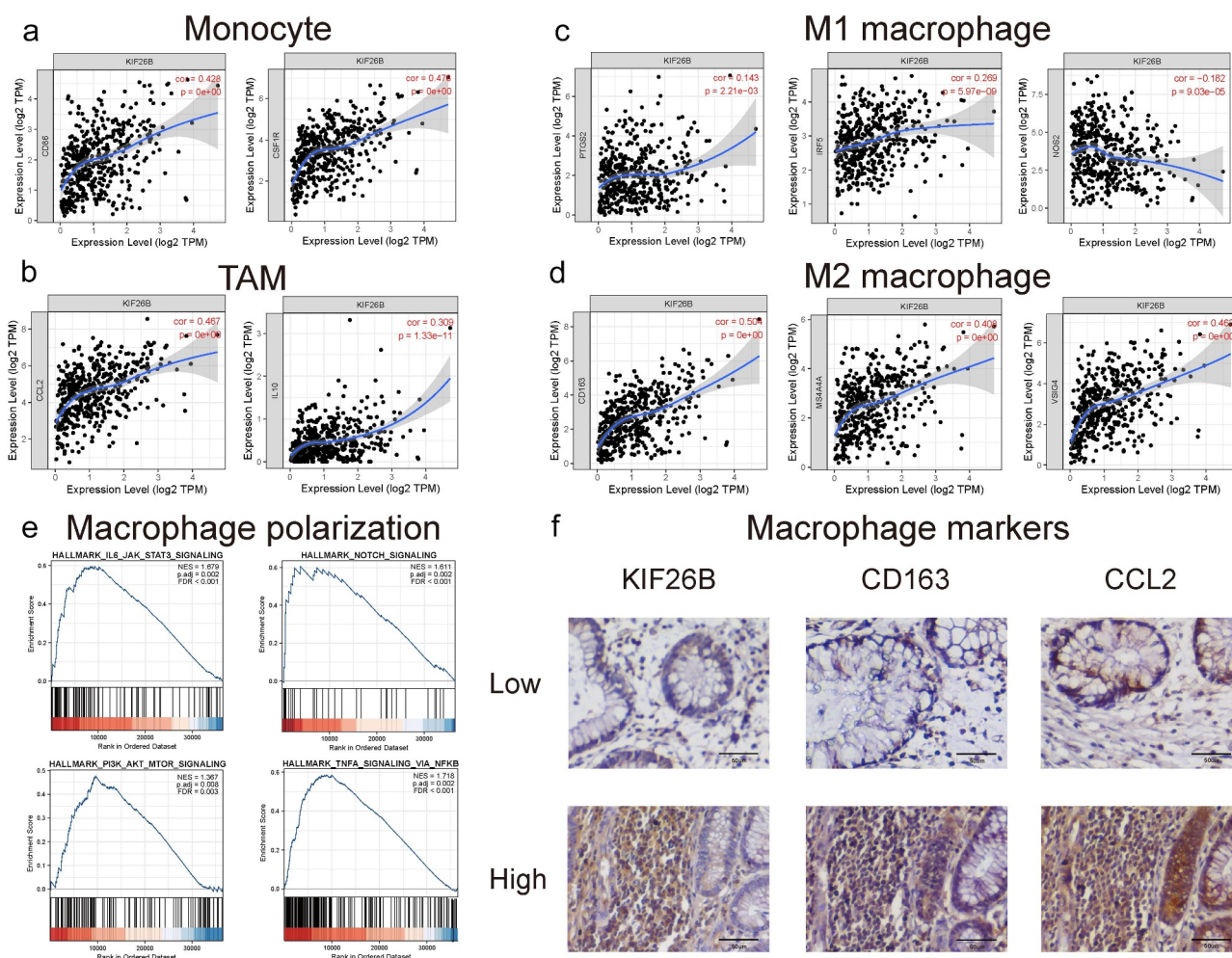


Figure 7. Relevance analysis between KIF26B expression and immunological marker set in COAD by TIMER. (a-d) the correlation between KIF26B expression and gene markers Monocyte (CD86, CSF1R) (a), TAM (CCL2, IL – 10) (b), M1 Macrophage (PTGS2, IRF5, NOS2) (c), M2 Macrophage (CD163, MS4A4A, VSIG4) (d). (e) KIF26B-related genes were significantly enriched in macrophage polarization-related pathways. (f) Validation of Macrophage-related markers between KIF26B^{low} and KIF26B^{high} group using IHC.

Table 3. The association between KIF26B expression and biomarkers of immune cells in COAD using GEPIA2.

Description	Gene markers	COAD			
		Tumor		Normal	
		r value	p value	r value	p value
TAM	CCL2	0.58	***	0.47	**
	CD68	0.42	***	-0.14	0.37
	IL10	0.47	***	-0.037	0.82
M1 Macrophage	INOS(NOS2)	-0.18	**	-0.064	0.69
	IRF5	0.32	***	-0.03	0.85
M2 Macrophage	COX2(PTGS2)	0.19	**	0.59	***
	CD163	0.57	***	-0.027	0.87
	VSIG4	0.57	***	-0.16	0.32
Monocyte	MS4A4A	0.53	***	-0.15	0.36
	CD86	0.49	***	-0.24	0.14
	CD115(CSF1R)	0.57	***	-0.013	0.93

Table 4. The association between KIF26B and CD163 expression.

Tissue sample	CD163 expression		<i>p</i> value	<i>r</i>
	Low	High		
KIF26B Low	15	5	0.001	0.523
KIF26B High	5	17		

Table 5. The association between KIF26B and CCL2 expression.

Tissue sample	CCL2 expression		<i>p</i> value	<i>r</i>
	Low	High		
KIF26B Low	17	4	0.001	0.667
KIF26B High	3	18		

Finally, we verified the correlation of KIF26B with two marker proteins of macrophages by immunohistochemistry, including CD163 and CCL2. As shown in Figure 7f, higher expression of KIF26B in colorectal cancer patients with high CD163 and CCL2 expression Table 4 and Table 5.

3.7 Association between KIF26B and immune checkpoints in COAD

Immune checkpoints, including PDCD1, CD274, and CTLA4, are closely involved in tumor immune escape. Our results found that the expression of KIF26B was closely related to immune checkpoint gene expression. As presented in Figure 8, KIF26B expression was significantly positively correlated with the expression of immune checkpoint-related genes in pan-cancer and COAD, including PDCD1 (Figure 8a,b), CD274 (Figure 8d,e), and CTLA4 (Figure 8g,h). This result was validated by our clinical specimens (Figure 8c,f,i).

4. Discussion

As the most common type of intestinal tract tumor, patients with COAD still have a poor prognosis. In recent years, the diagnosed population has tended to be younger. Thus, clarifying the molecular mechanism of colon cancer development and finding potential prognostic biomarkers are issues to be solved. Growing evidence suggested that KIF26B was involved in the initiation and progression of diverse tumors, especially COAD. However, the molecular mechanism of KIF26B and its relevance to immune cell infiltration in COAD have not been thoroughly studied and need further exploration.

Our study first performed a pan-cancer analysis of unusual KIF26B expression by OncoPrint and TCGA databases. Unpaired and paired specimens were subjected to difference analysis, and we found that KIF26B mRNA was increased significantly compared to those in normal controls. Similarly, the difference analysis of unpaired and paired tissue samples from GEO datasets and our clinical samples also confirmed the upregulated expression of KIF26B in COAD. The HPA database also indicated increased KIF26B expression at the protein level. Increased KIF26B expression may impact the underlying functions and mechanisms in COAD. Subgroup analysis demonstrated that KIF26B expression was positively related to T stage, N stage, and CEA levels but not M stage. Taken together, KIF26B was an underlying prognostic factor for colon cancer patients.

Noncoding RNAs (ncRNAs) do not encode a protein while they participate in gene expression regulation via a special mechanism. To identify the upstream regulatory miRNAs of KIF26B, candidate miRNAs binding to KIF26B were forecasted by StarBase, and 31 miRNAs were finally found. Then, miRNAs negatively correlated with KIF26B were filtered, and six miRNAs met this condition. After conducting expression analysis and survival analysis, we selected hsa-miR-500a-3p as the most promising downregulated tumor suppressor miRNA of KIF26B. According to our experimental results, we speculated that miRNAs may exert tumor suppressive effects by inhibiting the expression of KIF26B. Y. Liu et al. also suggested that hsa-miR-500a-3p could inhibit the proliferation and glycolysis of CRC cells [40].

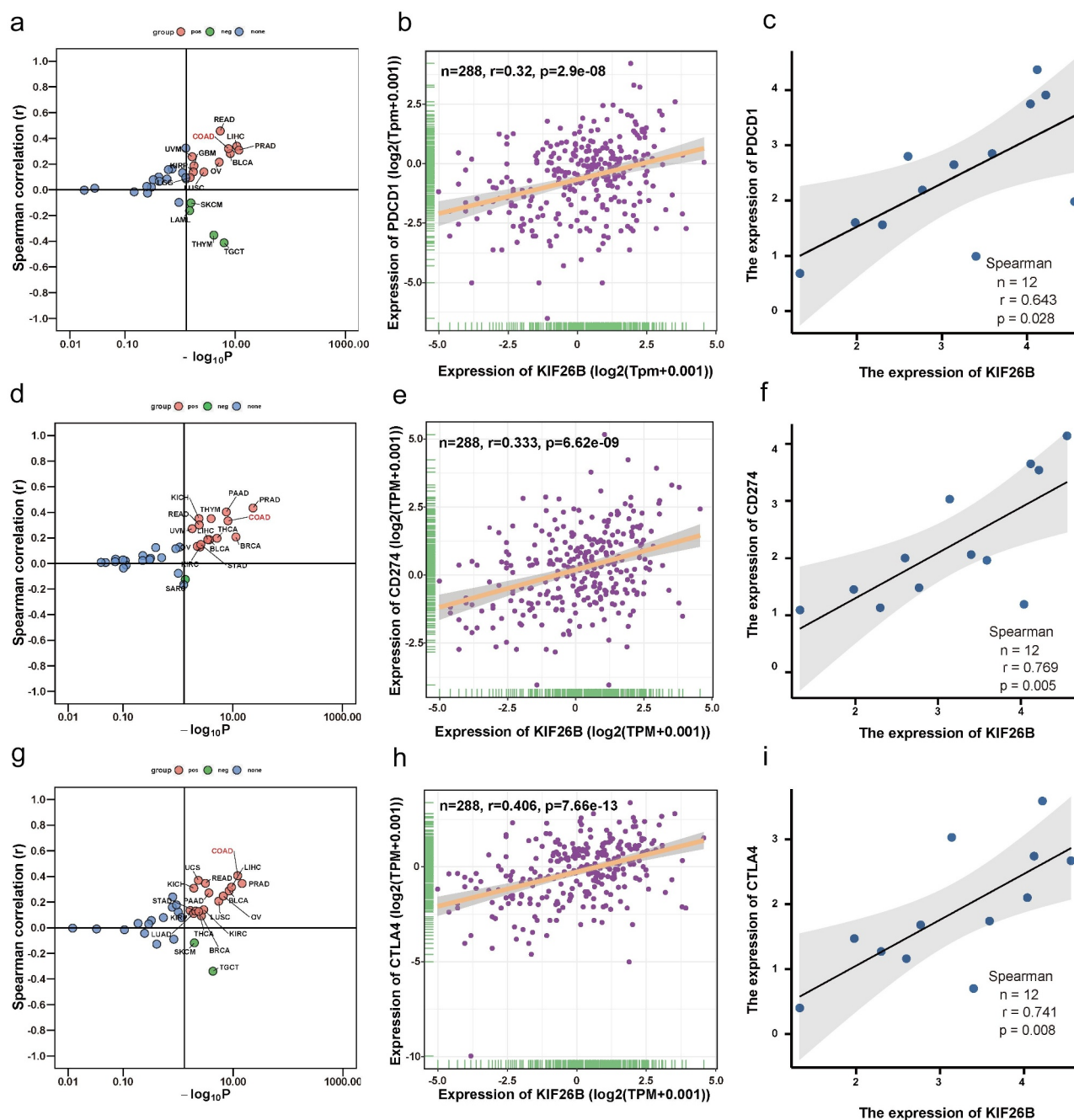


Figure 8. The relationship of KIF26B expression with PD CD1, CD274, and CTLA 4 expression in COAD. (a-c) Spearman correlation of KIF26B expression with PDCD1 expression in different types of human tumors, COAD, and clinical samples. (d-f) Spearman correlation of KIF26B expression with CD274 expression in different types of human tumors, COAD, and clinical samples. (g-i) Spearman correlation of KIF26B expression with CTLA 4 expression in different types of human tumors, COAD, and clinical samples.

According to the competitive endogenous RNA hypothesis, possible upstream lncRNAs should be negatively associated with hsa-miR-500a-3p or positively associated with KIF26B. Then, lncRNAs of hsa-miR-500a-3p precursors were forecasted, and 27 potential lncRNAs were obtained. By performing gene expression analysis, survival analysis, and relevance analysis, MIR4435-2HG was identified as the

most promising upregulated lncRNA in COAD. Our results also show that MIR4435-2HG may play a role in promoting tumor growth through competitive binding of hsa-miR-500a-3p. Previous studies had confirmed that MIR4435-2HG acted as an oncogene in Pan-cancer [41]. MIR4435-2HG also participated in colorectal cancer proliferation and migration via miR-206/YAP1 axis [42]. In general, MIR4435-2HG/

hsa-miR-500a-3p/KIF26B axis was constructed as a potential regulatory network in COAD.

Tumor microenvironment (TME), particularly immune microenvironment, plays a determinative role in cancer survival, progression, and tumor immune escape [43]. To further explore the relationship of KIF26B with immune microenvironment, we conducted gene-gene relevance analysis and found the co-expression relationship of KIF26B with genes encoding chemokine receptors, chemokines, immune suppression, and immune activation proteins in multiple tumors, especially COAD. Furthermore, we investigated the correlation between KIF26B expression and tumor purity and found that tumor purity was decreased with increased KIF26B expression, which indicated that patients with high expression of KIF26B have higher levels of immune infiltration. As expected, we discovered that KIF26B was positively related to multiple immune cells in COAD. Among these immune cells, the cell type most associated with KIF26B expression was macrophages. As the most typical tumor-infiltrating immune cells, macrophages played an essential role in the formation of TME. Thus, we speculated that KIF26B expression might impact patient prognosis by increasing the level of macrophage infiltration.

To investigate our speculation, we assessed the relationship of KIF26B expression with markers of infiltrating TAMs, M1 macrophages, M2 macrophages, and monocytes. As expected, the coefficients between KIF26B expression and the majority markers of macrophage subtype were positive in COAD. Previous studies confirmed that TAMs were key cells in the development of the TME and became the most promising therapeutic targets [44,45]. Our results revealed that TAMs had a positive correlation with KIF26B expression. We also found that KIF26B expression was closely related to M2 macrophages compared with M1 macrophages, which indicated that KIF26B expression may be associated with an increase in M2 macrophages. Research showed that M2 macrophages tend to exert an immune suppressive phenotype and were associated with poor prognosis [45]. In addition, we verified these results using the GEPIA2 database. KIF26B-related genes GSEA analysis and Immunohistochemical staining results also

showed that KIF26B expression was closely associated with increased infiltration of M2 type macrophages. In general, these results suggested that KIF26B expression may be associated with the formation of TME.

Immune checkpoints act as regulators of immune system and are crucial for maintaining immune homeostasis [46,47]. Tumor cells commonly hijack key Immune checkpoints to escape immune surveillance, and this mechanism becomes the basis of antitumor immunotherapy [48,49]. Thus, the association between KIF26B and immune checkpoints was evaluated. Our results suggested that upregulated KIF26B expression was positively correlated with PDCD1, CD274, and CTLA4. As an inhibitory receptor for immunomodulation, over-activation of these checkpoints will inevitably inhibit the activation of T cells, affect the anti-tumor effect of immune cells and cause immune escape of tumor cells. Thus, we speculated that KIF26B might be a potential immunotherapy target for COAD.

In summary, we validated abnormal KIF26B expression in various tumors and positively correlated KIF26B expression with unfavorable prognosis in COAD. MIR4435-2HG/hsa-miR-500a-3p/KIF26B axis was identified as an upstream regulatory mechanism in COAD. Moreover, our work demonstrated that KIF26B might exert its tumorigenic roles by increasing tumor immune cell infiltration, promoting the formation of TME, and upregulating immune checkpoint expression, thereby promoting tumor progression and proliferation. Of course, these results need further experimental verification.

Disclosure statement

No potential conflict of interest was reported by the authors.

Funding

This study was supported by the project of Suzhou Technology Bureau (SKY2021043, SLJ2022011), Suzhou Health Care Commission Medical Talent Project (GSWS2020037), Nuclear Technology Application Innovation Team, General Hospital of Nuclear Industry (XKTJ-HTD2021004).

Data availability statement

The original contributions presented in the study are openly available in TCGA database (<https://portal.gdc.cancer.gov/>) and GEO database (<https://www.ncbi.nlm.nih.gov/geo/>). Further inquiries can be directed to the corresponding authors.

Ethics statement

This study was approved by the institutional review board of the Second Affiliated Hospital of Soochow University Ethics Committee (Jiangsu province, China).

Author contributions

XY, JL, and ZL conceived and designed the study. XZ, BC, and ZL downloaded and processed data. ZL and XZ wrote the manuscript and helped with the validation. ZW, CZ, and CG wrote sections of the manuscript. All authors contributed to the article and approved the submitted version.

ORCID

Zhihong Liu  <http://orcid.org/0000-0002-8532-7170>
Xiaodong Yang  <http://orcid.org/0000-0001-7685-5011>

References

- [1] Sung H, Ferlay J, Siegel RL, et al. Global cancer statistics 2020: gLOBOCAN estimates of incidence and mortality worldwide for 36 cancers in 185 Countries. *Ca A Cancer J Clinicians*. 2021;71(3):209–249. doi: [10.3322/caac.21660](https://doi.org/10.3322/caac.21660)
- [2] Siegel RL, Miller KD, Goding Sauer A, et al. Colorectal cancer statistics, 2020. *CA A Cancer J Clin*. 2020;70(3):145–164. doi: [10.3322/caac.21601](https://doi.org/10.3322/caac.21601)
- [3] Dekker E, Tanis PJ, Vleugels JLA, et al. Colorectal cancer. *Lancet*. 2019;394(10207):1467–1480. doi: [10.1016/S0140-6736\(19\)32319-0](https://doi.org/10.1016/S0140-6736(19)32319-0)
- [4] Miki H, Setou M, Kaneshiro K, et al. All kinesin superfamily protein, KIF, genes in mouse and human. *Proc Natl Acad Sci U S A*. 2001;98(13):7004–7011. doi: [10.1073/pnas.111145398](https://doi.org/10.1073/pnas.111145398)
- [5] Thorn KS, Ubersax JA, Vale RD, Engineering the processive run length of the kinesin motor. *J Cell Bio* 151, 1093–1100 (2000). 5 doi: [10.1083/jcb.151.5.1093](https://doi.org/10.1083/jcb.151.5.1093)
- [6] Smith GA, Gross SP, Enquist LW, Herpesviruses use bidirectional fast-axonal transport to spread in sensory neurons. *Proc Natl Acad Sci U S A* 98, 3466–3470 (2001). 6 doi: [10.1073/pnas.061029798](https://doi.org/10.1073/pnas.061029798)
- [7] Hirokawa N, Takemura R, Kinesin superfamily proteins and their various functions and dynamics. *Exp Cell Res* 301, 50–59 (2004). 1 doi: [10.1016/j.yexcr.2004.08.010](https://doi.org/10.1016/j.yexcr.2004.08.010)
- [8] Vale RD, Fletterick RJ, The design plan of kinesin motors. *13*, 745–777 (1997). *Annu Rev Cell Dev Biol* 1 doi: [10.1146/annurev.cellbio.13.1.745](https://doi.org/10.1146/annurev.cellbio.13.1.745)
- [9] Hirokawa N, Noda Y, Okada Y, Kinesin and dynein superfamily proteins in organelle transport and cell division. *Curr Opin Cell Biol* 10, 60–73 (1998). 1 doi: [10.1016/S0955-0674\(98\)80087-2](https://doi.org/10.1016/S0955-0674(98)80087-2)
- [10] Sharp DJ, Rogers GC, Scholey JM, Microtubule motors in mitosis. *Nature* 407, 41–47 (2000). 6800 doi: [10.1038/35024000](https://doi.org/10.1038/35024000)
- [11] Liu X, Gong H, Huang K, Oncogenic role of kinesin proteins and targeting kinesin therapy. *Cancer Sci* 104, 651–656 (2013). 6 doi: [10.1111/cas.12138](https://doi.org/10.1111/cas.12138)
- [12] Rath O, Kozielski F, Kinesins and cancer. *Nat Rev Cancer* 12, 527–539 (2012). 8 doi: [10.1038/nrc3310](https://doi.org/10.1038/nrc3310)
- [13] Yu Y, Feng YM, The role of kinesin family proteins in tumorigenesis and progression: potential biomarkers and molecular targets for cancer therapy. *Cancer* 116, 5150–5160 (2010). 22 doi: [10.1002/cncr.25461](https://doi.org/10.1002/cncr.25461)
- [14] Karuna EP, Choi S, Scales M, et al. Identification of a WNT5A-Responsive degradation domain in the kinesin superfamily protein KIF26B. *Genes (Basel)*. 2018;9(4):196. doi: [10.3390/genes9040196](https://doi.org/10.3390/genes9040196)
- [15] Uchiyama Y, Sakaguchi M, Terabayashi T, et al. Kif26b, a kinesin family gene, regulates adhesion of the embryonic kidney mesenchyme. *Proc Natl Acad Sci U S A*. 2010;107(20):9240–9245. doi: [10.1073/pnas.0913748107](https://doi.org/10.1073/pnas.0913748107)
- [16] Terabayashi T, Sakaguchi M, Shinmyozu K, et al. Phosphorylation of Kif26b promotes its polyubiquitination and subsequent proteasomal degradation during kidney development. *PLoS ONE*. 2012;7(6):e39714. doi: [10.1371/journal.pone.0039714](https://doi.org/10.1371/journal.pone.0039714)
- [17] Gu S, Liang H, Qi D, et al., Knockdown of KIF26B inhibits breast cancer cell proliferation, migration, and invasion. *Onco Targets Ther* 11, 3195–3203 (2018). doi: [10.2147/OTT.S163346](https://doi.org/10.2147/OTT.S163346)
- [18] Teng Y, Guo B, Mu X, et al., KIF26B promotes cell proliferation and migration through the FGF2/ERK signaling pathway in breast cancer. *Biomed Pharmacother* 108, 766–773 (2018). doi: [10.1016/j.biopha.2018.09.036](https://doi.org/10.1016/j.biopha.2018.09.036)
- [19] Wang S, Zhang H, Liu H, et al., ELK1-induced up-regulation of KIF26B promotes cell cycle progression in breast cancer. *Med Oncol* 39, 15 (2022). 1 doi: [10.1007/s12032-021-01607-6](https://doi.org/10.1007/s12032-021-01607-6)
- [20] Li H, Shen S, Chen X, et al. MiR-450b-5p loss mediated KIF26B activation promoted hepatocellular carcinoma progression by activating PI3K/AKT pathway. *Cancer Cell Int*. 2019;19(1):205. doi: [10.1186/s12935-019-0923-x](https://doi.org/10.1186/s12935-019-0923-x)
- [21] Zhang H, Ma R-R, Wang X-J, et al. KIF26B, a novel oncogene, promotes proliferation and metastasis by activating the VEGF pathway in gastric cancer. *Oncogene*. 2017;36(40):5609–5619. doi: [10.1038/nc.2017.163](https://doi.org/10.1038/nc.2017.163)

- [22] Wang J, Cui F, Wang X, et al. Elevated kinesin family member 26B is a prognostic biomarker and a potential therapeutic target for colorectal cancer. *J Exp Clin Cancer Res.* 2015;34(1):13. doi: [10.1186/s13046-015-0129-6](https://doi.org/10.1186/s13046-015-0129-6)
- [23] Liu J, Lichtenberg T, Hoadley KA, et al. An Integrated TCGA pan-cancer clinical data resource to drive high-quality survival outcome analytics. *Cell.* 2018;173(2):400–416.e11. doi: [10.1016/j.cell.2018.02.052](https://doi.org/10.1016/j.cell.2018.02.052)
- [24] Uhlén M, Fagerberg L, Hallström BM, et al. Proteomics. Tissue-based map of the human proteome. *Science.* 2015;347(6220):1260419. doi: [10.1126/science.1260419](https://doi.org/10.1126/science.1260419)
- [25] Uhlen M, Zhang C, Lee S, et al., A pathology atlas of the human cancer transcriptome. *Science* 357, (2017). 6352 doi: [10.1126/science.aan2507](https://doi.org/10.1126/science.aan2507)
- [26] Rhodes DR, Kalyana-Sundaram S, Mahavisno V, et al. OncoPrint 3.0: genes, pathways, and networks in a collection of 18,000 cancer gene expression profiles. *Neoplasia.* 2007;9(2):166–180. doi: [10.1593/neo.07112](https://doi.org/10.1593/neo.07112)
- [27] Li T, Fan J, Wang B, et al. TIMER: a web server for comprehensive analysis of tumor-infiltrating immune cells. *Cancer Res.* 2017;77(21):e108–e110. doi: [10.1158/0008-5472.CAN-17-0307](https://doi.org/10.1158/0008-5472.CAN-17-0307)
- [28] Li T, Fu J, Zeng Z, et al. TIMER2.0 for analysis of tumor-infiltrating immune cells. *Nucleic Acids Res.* 2020;48(W1):W509–w514. doi: [10.1093/nar/gkaa407](https://doi.org/10.1093/nar/gkaa407)
- [29] Tang Z, Li C, Kang B, et al. GEPIA: a web server for cancer and normal gene expression profiling and interactive analyses. *Nucleic Acids Res.* 2017;45(W1):W98–W102. doi: [10.1093/nar/gkx247](https://doi.org/10.1093/nar/gkx247)
- [30] Kertesz M, Iovino N, Unnerstall U, et al., The role of site accessibility in microRNA target recognition. *Nat Genet* 39, 1278–1284 (2007). 10 doi: [10.1038/ng2135](https://doi.org/10.1038/ng2135)
- [31] Maragkakis M, Vergoulis T, Alexiou P, et al., DIANA-microT web server upgrade supports fly and worm miRNA target prediction and bibliographic miRNA to disease association. *Nucleic Acids Res* 39, W145–W148 (2011). suppl doi: [10.1093/nar/gkr294](https://doi.org/10.1093/nar/gkr294)
- [32] Betel D, Koppal A, Agius P, et al., Comprehensive modeling of microRNA targets predicts functional non-conserved and non-canonical sites. *Genome Bio* 11, R90 (2010). 8 doi: [10.1186/gb-2010-11-8-r90](https://doi.org/10.1186/gb-2010-11-8-r90)
- [33] Vejnar CE, Zdobnov EM, MiRmap: comprehensive prediction of microRNA target repression strength. *Nucleic Acids Res* 40, 11673–11683 (2012). 22 doi: [10.1093/nar/gks901](https://doi.org/10.1093/nar/gks901)
- [34] Anders G, Mackowiak SD, Jens M, et al., doRina: a database of RNA interactions in post-transcriptional regulation. *Nucleic Acids Res* 40, D180–D186 (2012). D1 doi: [10.1093/nar/gkr1007](https://doi.org/10.1093/nar/gkr1007)
- [35] Miranda KC, Huynh T, Tay Y, et al. A pattern-based method for the identification of MicroRNA binding sites and their corresponding heteroduplexes. *Cell.* 2006;126(6):1203–1217. doi: [10.1016/j.cell.2006.07.031](https://doi.org/10.1016/j.cell.2006.07.031)
- [36] Grimson A, Farh KK-H, Johnston WK, et al. MicroRNA targeting specificity in mammals: determinants beyond seed pairing. *Molecular Cell.* 2007;27(1):91–105. doi: [10.1016/j.molcel.2007.06.017](https://doi.org/10.1016/j.molcel.2007.06.017)
- [37] Li J-H, Liu S, Zhou H, et al., starBase v2.0: decoding miRNA-ceRNA, miRNA-ncRNA and protein–RNA interaction networks from large-scale CLIP-Seq data. *Nucl Acids Res* 42, D92–D97 (2014). D1 doi: [10.1093/nar/gkt1248](https://doi.org/10.1093/nar/gkt1248)
- [38] Subramanian A, Tamayo P, Mootha VK, et al. Gene set enrichment analysis: a knowledge-based approach for interpreting genome-wide expression profiles. *Proc Natl Acad Sci U S A.* 2005;102(43):15545–15550. doi: [10.1073/pnas.0506580102](https://doi.org/10.1073/pnas.0506580102)
- [39] Yu G, Wang LG, Han Y, et al. He, clusterProfiler: an R package for comparing biological themes among gene clusters. *OMICS* 16, 284–287 (2012). 5 doi: [10.1089/omi.2011.0118](https://doi.org/10.1089/omi.2011.0118)
- [40] Liu Y, Tang W, Ren L, et al. Activation of miR-500a-3p/CDK6 axis suppresses aerobic glycolysis and colorectal cancer progression. *J Transl Med.* 2022;20(1):106. doi: [10.1186/s12967-022-03308-8](https://doi.org/10.1186/s12967-022-03308-8)
- [41] Zhong C, Xie Z, Zeng LH, et al., MIR4435-2HG is a potential pan-cancer biomarker for diagnosis and prognosis. *Front Immunol* 13, 855078 (2022). doi: [10.3389/fimmu.2022.855078](https://doi.org/10.3389/fimmu.2022.855078)
- [42] Dong X, Yang Z, Yang H. Long non-coding RNA MIR4435-2HG promotes colorectal cancer proliferation and metastasis through miR-206/YAP1 axis. *Front Oncol.* 2020;10:160. doi: [10.3389/fonc.2020.00160](https://doi.org/10.3389/fonc.2020.00160)
- [43] Hinshaw DC, Shevde LA, The tumor microenvironment innately modulates cancer progression. *Cancer Res* 79, 4557–4566 (2019). 18 doi: [10.1158/0008-5472.CAN-18-3962](https://doi.org/10.1158/0008-5472.CAN-18-3962)
- [44] Komohara Y, Fujiwara Y, Ohnishi K. Tumor-associated macrophages: potential therapeutic targets for anti-cancer therapy. *Adv Drug Deliv Rev.* 2016;99:180–185. doi: [10.1016/j.addr.2015.11.009](https://doi.org/10.1016/j.addr.2015.11.009)
- [45] Lin Y, Xu J, Lan H, Tumor-associated macrophages in tumor metastasis: biological roles and clinical therapeutic applications. *J Hematol Oncol* 12, 76 (2019). 1 doi: [10.1186/s13045-019-0760-3](https://doi.org/10.1186/s13045-019-0760-3)
- [46] Liu Y, Zugazagoitia J, Ahmed FS, et al. Immune cell PD-L1 colocalizes with macrophages and is associated with outcome in PD-1 pathway blockade therapy. *Clin Cancer Res.* 2020;26(4):970–977. doi: [10.1158/1078-0432.CCR-19-1040](https://doi.org/10.1158/1078-0432.CCR-19-1040)
- [47] Sharpe AH, Wherry EJ, Ahmed R, et al., The function of programmed cell death 1 and its ligands in regulating autoimmunity and infection. *Nat Immunol* 8, 239–245 (2007). 3 doi: [10.1038/ni1443](https://doi.org/10.1038/ni1443)
- [48] Chen DS, Mellman I, Elements of cancer immunity and the cancer–immune set point. *Nature* 541, 321–330 (2017). 7637 doi: [10.1038/nature21349](https://doi.org/10.1038/nature21349)
- [49] Yi M, Zheng X, Niu M, et al. Combination strategies with PD-1/PD-L1 blockade: current advances and future directions. *Mol Cancer.* 2022;21(1):28. doi: [10.1186/s12943-021-01489-2](https://doi.org/10.1186/s12943-021-01489-2)